The Role of Respiratory Complex IV in Lifespan Length and Quality

Beatriz Castejon-Vega[1], Ignacio Fernandez-Guerrero[1], Kevin Myers[1], Tetsushi Kataura[2], Rhoda Stefanatos[1], Viktor I. Korolchuk[2], Alberto Sanz[1*]

[1] School of Molecular Biosciences, College of Medical, Veterinary and Life Sciences, University of Glasgow, G12 8QQ, Glasgow, United Kingdom.

[2] Biosciences Institute, Faculty of Medical Sciences, Newcastle University, Campus for Ageing and Vitality, NE4 5PL, Newcastle upon Tyne, United Kingdom.

Corresponding Author: Prof Alberto Sanz (Alberto.Sanzmontero@glasgow.ac.uk)

Abstract

Mitochondria play a pivotal role in lifespan regulation, though the underlying mechanisms remain elusive. As ageing progresses, damaged mitochondria with reduced ATP production and increased Reactive Oxygen Species (ROS) generation accumulate, yet mitochondrial depletion extends the lifespan of various animal models. Our previous research demonstrated that complex I (CI) activity during development but not adulthood is crucial for determining the lifespan of *Drosophila melanogaster*. Still, CI-deficient mitochondria do not generate excessive ROS, failing to recapitulate mitochondrial ageing. In this study, we focus on complex IV (CIV), whose depletion leads to the accumulation of "old-mitochondria", i.e. producing less ATP and more ROS. We reveal that CIV's role in longevity is more intricate than CI's, shaping lifespan through two "windows of opportunity". The first window, shared by CI and CIV, occurs during development. Small perturbations in CIV during development lead to the emergence of short-lived flies. These flies exhibit an adult phenotype reminiscent of mitochondrial-associated diseases, primarily characterised by their inability to store fat efficiently. Accordingly, partial complementation of CIV function using an alternative oxidase (AOX) restores molecular and physiological phenotypes. The second window emerges during fly senescence, where CIV deficiency curtails lifespan without hastening ageing—flies die earlier but not more rapidly. Notably, only the developmental phenotype is associated with TOR dysregulation and altered autophagy, emphasising that developmental dysfunction uniquely interferes with nutrient sensing and the main cellular recycling pathway. This study sheds light on the multifaceted role of mitochondrial complex IV in modulating lifespan, providing potential targets for interventions to foster healthy ageing.

Keywords

Ageing; Complex IV; *Drosophila*; Longevity; Mitochondria, TOR, autophagy

Abbreviations

AOX, Alternative Oxidase; Atg8, Autophagy-related 8; CI, Complex I; CIV, Complex IV; COX4, Cytochrome C Oxidase Subunit 4; COX5B, Cytochrome C Oxidase Subunit 5B; DEGs, Differentially Expressed Genes; EDTA, Ethylenediaminetetraacetic acid; EGTA, Ethylene Glycol-bis(β-aminoethyl ether)-N,N,N′,N′-tetraacetic acid; FC, Fold Change; GS, GeneSwitch; GSEA, Gene Set Enrichment Analysis; HEPES, 4-(2-hydroxyethyl)-1-piperazineethanesulfonic acid; KEGG, Kyoto Encyclopedia of Genes and Genomes; KCl, Potassium Chloride; KH2PO4, Potassium Dihydrogen Phosphate; MgCl2, Magnesium Chloride; mtROS, Mitochondrial Reactive Oxygen Species; NAD+, Nicotinamide Adenine Dinucleotide; NADH, Nicotinamide Adenine Dinucleotide (reduced); NaOH, Sodium Hydroxide; OXPHOS, Oxidative Phosphorylation; PCA, Principal Component Analysis; qPCR, Quantitative Polymerase Chain Reaction; RNAi, RNA Interference; ROS, Reactive Oxygen Species; RU-486, Mifepristone; TAG, Triacylglyceride; TMPD (N,N,N',N'-tetramethyl-p-phenylenediamine); TOR, Target of Rapamycin; TCA, Trichloroacetic Acid; Tris, Tris(hydroxymethyl)aminomethane; tubGS, tubulin-GeneSwitch.

1. Introduction

Mitochondria play a critical role in determining cellular fate and are believed to significantly impact organismal lifespan, though the precise nature of this relationship remains unclear (Lopez-Otin, Blasco et al. 2023). Defective mitochondria accumulate during ageing and can be found in the cells of patients suffering from degenerative diseases such as Parkinson's, Alzheimer's, and cancer (Wallace 2005). These mitochondria produce more toxic by-products known as free radicals and respire less efficiently (Graham, Stefanatos et al. 2022, Rimal, Tantray et al. 2023). Similarly, mutations in genes that encode mitochondrial proteins can cause fatal diseases that shorten lifespan (Gorman, Schaefer et al. 2015). Interestingly, inhibiting mitochondrial function can prevent the detrimental effects of cellular senescence in mammalian cells and extend lifespan in animal models ranging from worms to mice (Dillin, Hsu et al. 2002, Dell'agnello, Leo et al. 2007, Copeland, Cho et al. 2009, Correia-Melo, Marques et al. 2016).

To reconcile these seemingly opposite results, we generated *Drosophila melanogaster* fly models where mitochondrial function is interrupted selectively during development and adulthood or only during adulthood. Initially, we focused on mitochondrial complex I (CI) and demonstrated that developmental depletion of CI produces short-lived flies with severe metabolic problems (Stefanatos, Robertson et al. 2023)). However, restricted dysfunction of CI to adulthood produces long-lived flies without significant molecular or physiological alterations. Although short- and long-lived CI-depleted flies recapitulate and explain the opposite results of the literature (i.e. both reductions (Foriel, Renkema et al. 2019) and extensions associated with CI depletion (Owusu-Ansah, Song et al. 2013)), they are not a good model for aged mitochondria. We and others have shown that depletion of CI disrupts oxidative phosphorylation (OXPHOS) without increasing ROS levels (Graham, Stefanatos et al. 2022, Granat, Ranson et al. 2022, Rimal, Tantray et al. 2023). However, aged mitochondria are characterised by high levels of mtROS (Cocheme, Quin et al. 2011, Scialo, Sriram et al. 2016, Graham, Stefanatos et al. 2022), a phenotype observed when CIV is depleted, but not when CI is depleted (Graham, Stefanatos et al. 2022).

Here, we disrupt mitochondrial complex IV using RNA interference (RNAi) technology and find that CIV depletion provokes a different response than CI. While CI is only

necessary for adult lifespan regulation during development, CIV influences lifespan through two different "windows of opportunity". One is developmental and shared with CI, whereas the other occurs during senescence and is unique. Interestingly, only the developmental window of opportunity participates in the mitochondrial regulation of TOR signalling and its control over autophagy, indicating that CIV regulates biomolecular recycling in a context-specific manner.

2. Material and Methods

Fly husbandry

Drosophila melanogaster flies were cultured on a standard medium composed of 1% agar, 1.5% sucrose, 3% glucose, 3.5% dried yeast, 1.5% maize, 1% wheat germ, 1% soybean flour, 3% treacle, 0.5% propionic acid, and 0.1% Nipagin. Unless indicated otherwise, flies were nurtured at 25°C, and subjected to a 12-hour light/dark cycle, and primarily male flies were used in all experimentations. To express the various RNAi and transgenes involved in this research, the GeneSwitch (GS) system was used in conjunction with fluctuating concentrations of RU-486 (Abcam, ab120356). Flies used in all experiments were collected within a 48-hour period post-eclosion, employing CO_2 anaesthesia, and sustained at a population density of 20 flies per vial. The genotype and provenance of the fly strains engaged in this study are delineated in supplementary Table 1.

High-Resolution Respirometry

Mitochondrial respiration was assessed using an Oxygraph-2K (Oroboros Instruments). Ten adult flies were homogenised in an isolation buffer consisting of 250 mM sucrose, 5 mM Tris-HCl, and 2 mM EGTA (pH 7.4), subsequently diluted 10-fold with an assay buffer that included 120 mM KCl, 5 mM KH_2PO_4, 3 mM HEPES, 1 mM EGTA, 1 mM MgCl2, and 0.2% (w/v) BSA (pH 7.2). To estimate CIV-linked respiration, we used 0.5 mM TMPD (N,N,N',N'-tetramethyl-p-phenylenediamine) and 2 mM ascorbate, using 50 mM of sodium azide to inhibit CIV. The raw O2 flux data procured utilising Oroboros DatLab 7.0, was normalised to the protein concentration of each homogenate (expressed in picomoles of O2 per minute per milligram). Protein concentration was quantified via the Bradford assay.

Immunofluorescence and Confocal microscopy

Fat bodies from ~5 day old flies were dissected and fixed with 4% paraformaldehyde for 30 minutes at ambient temperature. Subsequent to rinsing in 1x PBS, tissues were incubated within a solution of 1x PBS complemented with 0.005% Saponin containing LipidTOXred at a dilution of 1:500 and DAPI at a dilution of 1:1000, for an hour at room temperature. Following this, samples underwent three 15-minute washing cycles in 1x PBS with 0.005% Saponin before being mounted on polylysine coated glass slides equipped with 13mm x 0.12mm spacers using Prolong Diamond. The mounted tissues were then visualised using a Leica SP8 DLS confocal microscope, and the resultant images were processed using ImageJ software.

NAD/NADH measurements.

The quantification of NAD+ and NADH in whole flies was performed according to the procedure described in (Kanamori, de Oliveira et al. 2018). Briefly, five replicates of 10 flies for NAD+ or 20 flies for NADH were homogenised using a motorised pestle. The homogenate was treated with 10% trichloroacetic acid (TCA) for NAD+ extraction or with 0.5 M sodium hydroxide (NaOH) and 5 mM EDTA for NADH extraction. The pH of each sample was adjusted to 8.0 using 1M Tris. The concentrations of NAD+ and NADH were inferred from the fluorescence intensity of resorufin, which was produced from an enzymatic cycling reaction incorporating resazurin, riboflavin 5'-monophosphate, alcohol dehydrogenase and diaphorase. Fluorescence intensity was measured every minute for an hour using a FLUOstar Omega (BMG Labtech). The determined NAD+ and NADH levels were normalised against a β-NAD (Sigma) standard curve and adjusted to protein concentration ascertained by the DC protein assay (BioRad).

RNA sequencing and differential expression analysis

Total RNA was extracted as previously described for qPCR gene expression analysis and submitted to the Department of Biochemistry, University of Cambridge, for quality control, Poly A selection, and library preparation using the TruSeq Stranded mRNA Library Prep. Sequencing was conducted on the Illumina NextSeq 2000 platform with NextSeq2000 100-cycles (2x50 bp) P3 sequencing. Read quality was assessed using FastQC v0.11.9, and Kallisto v0.48.0 was used to create an alignment index using the Drosophila melanogaster genome (BDGP6.32) and to map reads to the reference host transcriptome. The data were imported into R using the rhdf5 v2.44.0 and tidyverse

v2.0.0 packages, with Kallisto's abundance files imported via tximport v1.28.0 and annotations obtained using biomaRt v2.56.0. The data were curated by removing low-count transcripts and normalising counts with edgeR v3.42.2. Principal Component Analysis (PCA) was performed to identify the principal components explaining the most variance in the data. DEG analysis was conducted using Limma v3.56.1, with DEGs selected based on a fold change (FC) cutoff of >= or <= 1.5 and a false discovery rate (FDR) <0.05 unless otherwise stated. Functional enrichment analysis was undertaken using the GSEABase v16.0, clusterProfiler v4.8.1, and gprofiler2 v0.2.1 packages. Visualisations were primarily generated using ggplot2 v3.4.2.

Survival analysis.

Survival curves were constructed utilising GraphPad Prism 9 and scrutinised applying log-rank statistical methods. Each group comprised a minimum of 100 flies, with the experimentation replicated between 2-3 times. Lifespan at 25°C: Flies were relocated to fresh media every 2-3 days, with mortality rates recorded systematically. Hydrogen Peroxide Treatment: Flies aged between 3-5 days were transferred to vials comprising 5 ml of 1.5% agar, 5% sucrose, and 2.5% H2O2. Mortality was assessed at consistent intervals. Thermal Stress: Flies were cultured at 32°C and transferred to fresh media every 2-3 days, with mortality rates observed systematically. Starvation: Flies aged between 3-5 days were placed into vials containing 2ml of 1% agar. Mortality was recorded at regular intervals.

Statistical Analysis.

Data visualisation was done using GraphPad Prism 9 and the R programming language, depending on the requirements of each specific analysis. For statistical analysis, we used Analysis of Variance (ANOVA) or t-tests, with each test chosen based on the data distribution and experimental design. In cases where ANOVA indicated a significant difference, subsequent post-hoc tests were employed to determine the specific groups that differed. Survival curve comparisons were analysed using the Log-rank test, a non-parametric test that compares survival rates between two or more groups. All statistical analyses were performed with a level of significance set at a p-value of less than 0.05, and all data are presented as mean ± SEM unless otherwise specified.

TAG assay.

15 male adult flies, *per* sample, were weighed and subsequently homogenised in Tet buffer (comprising 10 mM Tris, 1 mM EDTA, pH 8.0 with 0.1% v/v Triton-X-100) employing glass beads and an OMNI Bead Ruptor. Post-homogenisation, samples were incubated at 72°C for 20 min and then centrifugated at 13,000 rcf for 1 minutes at 4ºC. The resulting supernatant was then incubated at 72ºC for 15 minutes. Subsequently, a mixture of 3 µl of the sample and glycerol standards was added to 300 µl of ThermoFisher Infinity Triglyceride reagent and left to incubate for 15 minutes at 37ºC. Absorbance was measured at 540nm utilising a Multiskan FC (ThermoFisher). The glycerol standard curve, combined with the weight and number of flies, was employed to compute the Triacylglycerol (TAG) content per milligram per fly.

Western blot.

Five replicates of 10 flies were lysed in RIPA buffer (Sigma-Aldrich) supplemented with Halt protease and phosphatase inhibitor cocktail (ThermoFisher Scientific) using a motorised pestle. Whole fly lysates were then centrifuged at 4ºC at 16,13,000 rcf for 10 min to remove insoluble protein. Protein concentrations were measured using DC protein assay (BioRad) abd a GloMax plate-reader (Promega). Samples were prepared by boillling with 2x Laemmli sample buffer (BioRad) at 100ºC for 5 min in the presence of 2.5% β-mercaptoethanol (Sigma-Aldrich). Equal amounts of protein (40 µg) were subjected to SDS-PAGE with 8% or 15% Tris-Glycine gels and transferred to Immobilon-P PVDF membranes (Millipore) using a TransBlot SD Semi-Dry Transfer Cell (BioRad). Membranes were then blocked with 5% milk in PBS with Tween-20 for 30 min at room temperature and incubated with primary antibodies diluted in 5% BSA or 5% milk solution supplemented with 0.02% sodium azide overnight at 4ºC. Secondary antibodies conjugated to horseradish peroxidase (HRP) for rabbit (Sigma-Aldrich) or mouse (Sigma-Aldrich) were used at 1:5,000 dilution for 1 h at room temperature. Chemiluminescence detection was achieved using Clarity Western ECL Substrate (BioRad) and a LAS-4000 system (Fujifilm). The following primary antibodies were used: α-Tubulin (DSHB, 12G10, 1:10,000); Atg8 (gift from Dr Ivana Bjedov, 1:1,000); p70 S6K (Santa Cruz, sc-230, 1:1,000); phospho-p70 S6K (Cell Signalling, 9209, 1:1,000); Ref(2)P (Abcam, ab178440, 1:1,000). Densitometry analyses on immunoblots were performed using Fiji (ver. 1.53c).

3. Results

3.1. Developmental depletion of respiratory CIV profoundly reduces adult lifespan.

To investigate the role of CIV on the adult lifespan of *Drosophila*, we employed RNAi against two different subunits of the mentioned respiratory complex: COX5B and COX4. We used the inducible tubulin-GeneSwitch (tubGS) driver to trigger mitochondrial dysfunction during either the developmental stage or adulthood (Figure 1A). We observed that initiating the knockdown of COX5B and COX4 during development resulted in massively short-lived flies (~68% and ~57% for COX5B and COX4, respectively) (Figure 1B, C). However, compared to a control group with normal CIV levels, the reduction in lifespan was relatively moderate for COX5B (~20%) and even less pronounced for COX4 (~11%), specifically when their respective RNAis were exclusively triggered during adulthood. In both lines, flies where RNAi was induced only in adulthood were clearly long-lived compared to the short-lived lines where RNAi was induced during development. Furthermore, we noted a direct proportionality between the degree of lifespan reduction and the induction of mitochondrial dysfunction during development; the higher the concentration of RU-486 in the fly food, the more dramatic the shortening of the adult lifespan was (Figure S1A).

The mortality analysis of the survival curves indicated that short-lived flies had an earlier but slower death rate compared to long-lived and control flies (Figure S1B,C). This trend was observed for both COX5B and COX4 subunits. However, no consistent pattern was observed among long-lived flies between the two studied subunits. Long-lived COX5B flies exhibited an earlier but slower mortality rate compared to controls, while COX4 flies showed a slightly delayed but faster mortality rate. These findings suggest that depleting CIV does not inherently accelerate ageing. However, mortality rates may increase, particularly when targeting CIV during development, leading to earlier mortality. As

anticipated, RU-486 did not influence the survival of adult control flies possessing normal levels of CIV (Figure S1D).

To verify that our experimental manipulations had the intended impact on CIV levels, we employed both quantitative PCR (qPCR) and high-resolution respirometry. As anticipated, we detected a decrease in the mRNA levels of the target genes during development, but only in those flies that were fed with RU-486. Given that different RNAi constructs exhibit varied efficacies, it was not unexpected that a decrease in the target gene was observed in pupae for COX5B, whilst the decrease was already significant in L3 for the short-lived COX4 (Figure 1D, E). Importantly, we observed no difference in the levels of either COX5B or COX4 in adults, regardless of whether they were short- or long-lived (Figure 1F, G). Likewise, we detected no differences in mitochondrial oxygen consumption between short- and long-lived individuals (Figure 1H, I). The latter observation is particularly noteworthy, as it suggests that a decrease in the activity of CIV exceeding 50% does not significantly accelerate ageing. However, it can lead to an increase in early mortality, thereby reducing lifespan. The degree of this effect is contingent upon the specific subunit target.

3.2. Developmental depletion of CIV triggers transcriptomic reconfiguration, dysregulating fatty acid metabolism in adults.

To gain insight into the impact of CIV depletion on lifespan, we conducted a transcriptome analysis of short- and long-lived flies (Figure 2A). Principal Component Analysis (PCA) revealed a distinct separation between the short- and long-lived groups compared to the controls and variation within each group (Figure 2B). As expected, the two control groups with and without RU-486 feeding during development clustered together. To further elucidate the effect of CIV disruption during development on adult

lifespan, we compared short- and long-lived COX5B flies. Through a volcano plot representing differentially expressed genes (DEGs), we observed a more significant number of downregulated than upregulated genes (Figure 2C). Consistently with expectations, no DEGs were found when comparing short- and long-lived control flies (Figure S2A). Subsequently, we conducted Gene Ontology (GO) analysis using the identified DEGs (Figure 2D). Intriguingly, metabolic pathways emerged as the predominant topic across all examined categories, including Biological Process, Cellular Component, Molecular Function or KEGG. Of particular significance were the observed alterations in fatty acid metabolism. Our results indicate a pronounced downregulation of bioenergetics pathways in flies caused by a mild depletion of CIV levels during development.

Next, we conducted a volcano plot analysis using the FlyAtlas (Leader, Krause et al. 2018) dataset to pinpoint the tissues most impacted by developmental CIV depletion. This approach involved comparing the expression levels of the most highly expressed genes in various fly tissues in short- and long-lived COX5B flies (Figure 2E). The fat body, heart, carcass, and Malpighian tubules were the most impacted tissues. Genes were mainly downregulated except for the Malpighian tubules, where DEGs were predominantly upregulated. Most genes fell into the non-significantly expressed category for the other tissues, except for the midgut (Figure S2B). These results support the notion that central tissues involved in fatty acid metabolism, such as the heart and particularly the fat body, are greatly affected by mitochondrial dysfunction during development.

These findings align with our previous study on flies depleted in CI (Stefanatos, Robertson et al. 2023). Thus, we decided to compare the DEGs identified in models where either CI or CIV were depleted during development (Figure 2F). Interestingly, a substantial overlap was observed in the downregulated gene category, while the number

of commonly upregulated genes was more modest. Additionally, the shared metabolic pathways (e.g. fatty acid metabolism) and affected tissues (e.g. fat body) were highly consistent between the two models(Stefanatos, Robertson et al. 2023). This points towards a common response to mitochondrial dysfunction, consistently leading to the downregulation of genes engaged in energy metabolism, regardless of the specific respiratory complexes impacted.

Finally, upon manual inspection, we discovered that many ribosomal genes not meeting our 1.5 FC cutoff were significantly downregulated in the short-lived COX5B individuals. To statistically support the former, we performed Gene Set Enrichment Analysis (GSEA), which revealed a significant alteration in "Reactome Eukaryotic Translation and Elongation" and "KEGG Ribosome" in the short-lived individuals (Figure S2C, D), indicating a reduction in protein translation and cellular growth. In summary, transcriptomic analysis unveiled a pronounced inhibition of energetic metabolism, with the fat body being particularly affected, along with a mild yet significant decrease in the expression of genes involved in mRNA translation.

3.3. Developmental depletion of CIV disrupts fat storing and interrupts TOR signalling in adults.

We performed molecular and physiological experiments to confirm the nature of the metabolic alterations suggested by transcriptomic analyses. Firstly, we examined the fat body and observed the absence of lipids using LipidTox staining exclusively in the short-lived individuals (Figure 3A), suggesting that proper CIV levels are unnecessary for adult fat metabolism. Consistent with the fat body images, triacylglycerol (TAG) levels were significantly reduced in short-lived COX5B individuals (Figure 3B), making them particularly susceptible to starvation (Figure 3C). None of these phenotypes were

observed in the controls fed with RU-486 during development (Figure S3A ,B). Short-lived individuals were more sensitive to other stresses (namely oxidative and thermal stress), too, when compared to long-lived COX5B flies (Fig S3C, E), whereas no differences were observed between short- and long-lived controls (Figure S3D, F). The former observations indicate a general reduction in the organism's capacity to confront physiological stress. However, this phenomenon appears to be directly associated only with CIV levels during developmental stages.

We hypothesised that the energetic crisis observed in short-lived COX5B individuals would likely cause alterations in the activity of the cell's primary nutrient-sensing pathway, i.e., Target of Rapamycin (TOR) (Bjedov and Partridge 2011). This hypothesis was further supported by the diminished translation shown in the GSEA analysis of the short-lived flies' transcriptome. We quantified the phosphorylated and unphosphorylated S6 kinase levels and noticed a significant reduction in phosphorylated S6 kinase, suggesting a decrease in TOR signalling (Figure 3D, E). We reckoned that such a reduction in Tor signalling would impact autophagy since both are tightly connected (Bjedov, Toivonen et al. 2010). For further substantiation of the former, we assessed the levels of two autophagy markers: Ref(2)P and Atg8 (lipidated (Atg8-II) and unlipidated (Atg8-I) (Figure 3F). A remarkable increase in Ref(2)P and Atg8-II was detected, implying upregulated autophagy occurring exclusively in the short-lived COX5B individuals (Figure 3G). Lastly, we chose to measure the levels of NADH and NAD+, which have been reported to exhibit alterations in models where autophagy regulation is compromised (Kataura, Sedlackova et al. 2022), as well as in mitochondrial diseases (Pirinen, Auranen et al. 2020). Strikingly, we noticed a pronounced depletion in both, restricted to the short-lived COX5B flies (Figure 3H & S3G), i.e. depletion of CIV limited to adulthood did not change the redox state or the levels of NADH. In summary, our results highlighted an intriguing link

between the amount of CIV, the cell's primary nutrient-sensing pathway (TOR signalling), and the major proteolytic system (autophagy). Surprisingly, this connection exists only when CIV is depleted during development; there is no direct correlation between TOR/autophagy/NADH and adult CIV levels.

3.4 Targeted rescue of mitochondrial function during development improves energetic balance in adults.

To substantiate the hypothesis that developmental mitochondrial functionality is crucial for achieving healthy, prolonged lifespans, we performed experiments to complement CIV function exclusively during development, taking advantage of the GS system (Figure 4A). We utilised fly lines expressing an alternative oxidase (AOX) from *Ciona intestinalis* due to AOX's ability to counteract the lethality induced by developmental CIV depletion (Kemppainen, Rinne et al. 2014). Initially, we produced the transcriptome of flies expressing AOX solely during development (AOX active in Figure 4) in CIV-depleted flies. PCA delineated a clear distinction between short-lived COX5B flies expressing AOX during development or not, but as expected; this distinction was not present in long-lived counterparts (Figure 4B). Next, we identified a subset of genes that AOX significantly rescued (Figure S4A) and proceeded with GO analysis. Our results revealed an enrichment of genes associated with fatty acid metabolism among those whose expression was restored (Figure 4C). Moreover, we noted that the expression of numerous genes, such as Fbp1 and Fbp2, exclusively expressed in the larval fat body in wild-type flies, and aberrantly expressed in short-lived COX5B adults, was rectified by developmental AOX expression (Figure 4D, E). However, the rescue was not universal, with many genes involved in metabolic and other cellular processes remaining unchanged by AOX expression.

Next, we proceeded with physiological and molecular assays to confirm the impact of partial transcriptomic reprogramming. Starvation experiments demonstrated that AOX significantly enhanced the survival rate of short-lived flies (Figure 4F). No differences were observed among long-lived COX5B depleted flies, irrespective of AOX presence (Figure S4B). Importantly, continuous AOX expression throughout development and adulthood did not extend lifespan beyond that achieved by developmentally restricted expression (Figure S4C and D), endorsing our hypothesis of development as the pivotal stage for mitochondrial function in stress adaptation. Finally, imaging of total lipid levels in the fat body (Figure S4E) and TAG measurements (Figure S4F) in whole flies showed a partial rescue correlating with the transcriptomic and physiological experiments' output. In conclusion, our experiments show that partial recovery of mitochondrial function during development is sufficient to effectively reprogramme metabolism, bolstering starvation adaptation via enhanced fatty acid storage in adults.

4. Discussion

Our investigation sheds light on the central role of CIV in lifespan regulation, underscoring two distinct "windows of opportunity" where its influence is exerted. The initial window appears during developmental stages, with a secondary one manifesting during senescence. We show that the adult lifespan is reduced proportionately to the extent of CIV disruption experienced during development (Figure 1). The dramatic effect of developmental CIV disruption contrasts with the moderate lifespan reduction observed when CIV depletion is limited to adulthood. We previously reported that CI depletion during development produced a similar phenotype (Stefanatos, Robertson et al. 2023) . However, adult-limited CI depletion did not alter survival. This surprising finding indicates that different respiratory complexes participate differently in regulating adult lifespan. Accordingly, a recent paper (Lesner, Wang et al. 2022) reports that CIV is essential to

maintain metabolic balance in the adult mouse liver, but CI is dispensable, which agrees with our conclusions.

The mortality analysis of lifespan indicates a unique death rate pattern in short-lived CIV flies. They began to die earlier, but their death rate was slower, suggesting a distinctive interplay between developmental mitochondrial function, adult survival, and death dynamics. Our new findings and previous ones regarding CI (Stefanatos, Robertson et al. 2023) highlight the significance of maintaining mitochondrial function during development, as it potentially sets the course for future health and longevity. This concurs with earlier research in worms and flies, where an increase in ROS levels during development extended lifespan (Obata, Fons et al. 2018, Bazopoulou, Knoefler et al. 2019). In our case, the primary role of ROS can be discounted since we and others have observed contrasting effects of CI and CIV depletion on them (Graham, Stefanatos et al. 2022, Granat, Ranson et al. 2022, O'Hanlon, Tweedy et al. 2022). Interpreting the role of CIV during adulthood is more challenging, as we did not observe a consistent pattern. In all experiments, the lifespan of long-lived CIV flies was reduced. However, flies started to die earlier yet slower than controls when COX5B was targeted, while the opposite was observed when targeting COX4 (Figure 1). Regardless, these experiments demonstrate that a reduction in CIV activity by more than 50% does not necessarily accelerate ageing, although it consistently shortens the median lifespan.

Molecular characterisation of the short-lived COX5B flies (Figure 2) revealed how developmental depletion of CIV substantially altered the adult transcriptome, causing significant dysregulation of energetic metabolism, particularly affecting fatty acid homeostasis. This is similar to what we observed in CI-depleted flies (Stefanatos, Robertson et al. 2023), indicating that early-life mitochondrial dysfunction can significantly affect metabolic pathways, particularly lipid homeostasis, thereby inducing

lasting physiological effects in adults. Notably, the impact was most pronounced in the fat body, a critical tissue for energy storage and metabolism, underscoring the crucial interplay between mitochondrial dysfunction, energy homeostasis, and ageing.

Given the profound metabolic reprogramming of the adult transcriptome, the low resistance of short-lived CIV flies to starvation does not come as a surprise. This is further accentuated by the reduced capacity of the fat body to store lipids and the depleted levels of TAG detected in short-lived individuals (Figure 3). More striking, however, is the interruption in TOR signalling and dysregulation of autophagy present solely in short-lived individuals. Alterations in TOR signalling have been previously associated with CI (Johnson, Yanos et al. 2013, Wang, Mouser et al. 2016) , albeit in the reverse direction as reported here, i.e., elevated TOR signalling. We do not attribute these opposing results to the respiratory complex targeted, as we observe the same when CI is depleted. Other models of mitochondrial dysfunction, i.e. mutations in *tko* (that encodes the mitoribosomal protein S12), show a similar decrease in TOR signalling (Kemppainen, George et al. 2016) as the one we report here. Thus, reconciling these results remains an open question. In line with the reduction in TOR signalling, we noted a substantial increase in autophagy markers associated exclusively with developmental CIV depletion. Both phenomena might respond to the short-lived individuals' inability to store fat, compelling them to utilise other fuels by activating autophagy. Notably, the long-lived COX5 individuals did not exhibit any of these issues, thereby precluding a direct link between CIV and TOR signalling or autophagy.

Experiments involving the rescue of CIV function by expressing AOX during development support the idea that development is the critical period where mitochondria determine lifespan (Figure 4). The expression of AOX partially ameliorates the transcriptomic and physiological changes caused by CIV depletion. This effect is

particularly noticeable in restoring metabolic pathways related to lipid storage and improving fat body function. The partial rescue brought about by AOX can be attributed to two primary factors. First, there are constraints in achieving high levels of AOX expression. High doses of RU-486, necessary to significantly boost AOX levels, are lethal to the short-lived COX5B not treated with AOX. Second, AOX only partially complements the functionality of CIV (Fernandez-Ayala, Sanz et al. 2009). Despite these limitations, AOX expression during development still substantially improves the physiological state of CIV-depleted individuals.

In summary, our research provides significant insights into the role of mitochondria in ageing. Firstly, it reinforces the idea of a developmental 'window of opportunity', during which the mitochondrial function must remain intact for a healthy and long life. Even minor disturbances during this critical phase can significantly impact adult survival. Secondly, unlike CI, adult CIV activity appears to influence the lifespan of adult flies. However, our findings do not suggest that adult CIV depletion hastens ageing; it increases the probability of earlier death. Finally, although our results cannot be directly translated to humans, they suggest that mitochondrial diseases must be addressed either early during development (Hyslop, Blakeley et al. 2016) or—if in adulthood—through strategies focused on reprogramming specific tissues rather than simply restoring mitochondrial function (Jain, Zazzeron et al. 2019). Similarly, studying mitochondrial function in adults necessitates careful controls to eliminate the effects from developmental stages. Thus, our work has highlighted the intricate interplay between developmental and adult mitochondrial function and lifespan and illuminated potential therapeutic pathways for mitochondrial disorders.

5. Acknowledgements

This research was supported by two BBSRC grants (BB/R008167/2 & BB/W006774/1) and a Wellcome Senior Research Fellowship (212241/A/18/Z) to A.S. R.S. was supported by a Sir Henry Wellcome Postdoctoral Fellowship (204715/Z/16/Z). T.K. was supported by two fellowships from the Uehara Memorial Foundation and International Medical Research Foundation. I.F.G was supported by an MVLS DTP studentship. V.I.K. acknowledges support by the H2020 Twinning project RESETageing (GA 952266).

6. Notes on authors' contributions

B.C-V. performed lifespan experiments, qPCR, high-resolution respirometry, confocal imaging, and stress experiments.

I.F-G. generated the transcriptomics data.

K.M. provided technical support in lifespan, qPCR, and stress experiments.

T.K. and V.I.K. conducted western-blot analysis and measurements of NADH/NAD+ levels.

R.S. performed confocal imaging and high-resolution respirometry experiments and assisted with qPCR, stress experiments and transcriptomics analysis.

A.S. designed and supervised the project, wrote the first draft of the manuscript, performed transcriptomic analysis, created the figures, and wrote the initial version.

All authors contributed to analysing and discussing the results and revised the manuscript.

7. Ethical Statement/Conflict of Interest

V.I.K is a Scientific Advisor for Longaevus Technologies. Other authors declare no competing interests.

8. References

Bazopoulou, D., D. Knoefler, Y. Zheng, K. Ulrich, B. J. Oleson, L. Xie, M. Kim, A. Kaufmann, Y. T. Lee, Y. Dou, Y. Chen, S. Quan and U. Jakob (2019). "Developmental ROS individualizes organismal stress resistance and lifespan." Nature **576**(7786): 301-305.

Bjedov, I. and L. Partridge (2011). "A longer and healthier life with TOR down-regulation: genetics and drugs." Biochem Soc Trans **39**(2): 460-465.

Bjedov, I., J. M. Toivonen, F. Kerr, C. Slack, J. Jacobson, A. Foley and L. Partridge (2010). "Mechanisms of life span extension by rapamycin in the fruit fly Drosophila melanogaster." Cell Metab **11**(1): 35-46.

Cocheme, H. M., C. Quin, S. J. McQuaker, F. Cabreiro, A. Logan, T. A. Prime, I. Abakumova, J. V. Patel, I. M. Fearnley, A. M. James, C. M. Porteous, R. A. Smith, S. Saeed, J. E. Carre, M. Singer, D. Gems, R. C. Hartley, L. Partridge and M. P. Murphy (2011). "Measurement of H2O2 within living Drosophila during aging using a ratiometric mass spectrometry probe targeted to the mitochondrial matrix." Cell Metab **13**(3): 340-350.

Copeland, J. M., J. Cho, T. Lo, Jr., J. H. Hur, S. Bahadorani, T. Arabyan, J. Rabie, J. Soh and D. W. Walker (2009). "Extension of Drosophila life span by RNAi of the mitochondrial respiratory chain." Curr Biol **19**(19): 1591-1598.

Correia-Melo, C., F. D. Marques, R. Anderson, G. Hewitt, R. Hewitt, J. Cole, B. M. Carroll, S. Miwa, J. Birch, A. Merz, M. D. Rushton, M. Charles, D. Jurk, S. W. Tait, R. Czapiewski, L. Greaves, G. Nelson, Y. M. Bohlooly, S. Rodriguez-Cuenca, A. Vidal-Puig, D. Mann, G. Saretzki, G. Quarato, D. R. Green, P. D. Adams, T. von Zglinicki, V. I. Korolchuk and J. F. Passos (2016). "Mitochondria are required for pro-ageing features of the senescent phenotype." EMBO J **35**(7): 724-742.

Dell'agnello, C., S. Leo, A. Agostino, G. Szabadkai, C. Tiveron, A. Zulian, A. Prelle, P. Roubertoux, R. Rizzuto and M. Zeviani (2007). "Increased longevity and refractoriness to Ca(2+)-dependent neurodegeneration in Surf1 knockout mice." Hum Mol Genet **16**(4): 431-444.

Dillin, A., A. L. Hsu, N. Arantes-Oliveira, J. Lehrer-Graiwer, H. Hsin, A. G. Fraser, R. S. Kamath, J. Ahringer and C. Kenyon (2002). "Rates of behavior and aging specified by mitochondrial function during development." Science **298**(5602): 2398-2401.

Fernandez-Ayala, D. J., A. Sanz, S. Vartiainen, K. K. Kemppainen, M. Babusiak, E. Mustalahti, R. Costa, T. Tuomela, M. Zeviani, J. Chung, K. M. O'Dell, P. Rustin and H. T. Jacobs (2009). "Expression of the Ciona intestinalis alternative oxidase (AOX) in Drosophila complements defects in mitochondrial oxidative phosphorylation." Cell Metab **9**(5): 449-460.

Foriel, S., G. H. Renkema, Y. Lasarzewski, J. Berkhout, R. J. Rodenburg, J. A. M. Smeitink, J. Beyrath and A. Schenck (2019). "A Drosophila Mitochondrial Complex I Deficiency Phenotype Array." Front Genet **10**: 245.

Gorman, G. S., A. M. Schaefer, Y. Ng, N. Gomez, E. L. Blakely, C. L. Alston, C. Feeney, R. Horvath, P. Yu-Wai-Man, P. F. Chinnery, R. W. Taylor, D. M. Turnbull and R. McFarland (2015). "Prevalence of nuclear and mitochondrial DNA mutations related to adult mitochondrial disease." Ann Neurol **77**(5): 753-759.

Graham, C., R. Stefanatos, A. E. H. Yek, R. V. Spriggs, S. H. Y. Loh, A. H. Uribe, T. Zhang, L. M. Martins, O. D. K. Maddocks, F. Scialo and A. Sanz (2022). "Mitochondrial ROS signalling requires uninterrupted electron flow and is lost during ageing in flies." Geroscience.

Granat, L., D. Ranson, E. Hamer, R. P. Chakrabarty, F. Mattedi, L. Fort-Aznar, F. Hirth, S. T. Sweeney, A. Vagnoni, N. S. Chandel and J. M. Bateman (2022). "Yeast NDI1 reconfigures neuronal metabolism and prevents the unfolded protein response in mitochondrial complex I deficiency." bioRxiv: 2022.2009.2022.509020.

Hyslop, L. A., P. Blakeley, L. Craven, J. Richardson, N. M. Fogarty, E. Fragouli, M. Lamb, S. E. Wamaitha, N. Prathalingam, Q. Zhang, H. O'Keefe, Y. Takeda, L. Arizzi, S. Alfarawati, H. A. Tuppen, L. Irving, D. Kalleas, M. Choudhary, D. Wells, A. P. Murdoch, D. M. Turnbull, K. K. Niakan and M. Herbert (2016). "Towards clinical application of pronuclear transfer to prevent mitochondrial DNA disease." Nature **534**(7607): 383-386.

Jain, I. H., L. Zazzeron, O. Goldberger, E. Marutani, G. R. Wojtkiewicz, T. Ast, H. Wang, G. Schleifer, A. Stepanova, K. Brepoels, L. Schoonjans, P. Carmeliet, A. Galkin, F. Ichinose, W. M. Zapol and V. K. Mootha (2019). "Leigh Syndrome Mouse Model Can Be Rescued by Interventions that Normalize Brain Hyperoxia, but Not HIF Activation." Cell Metab **30**(4): 824-832 e823.

Johnson, S. C., M. E. Yanos, E. B. Kayser, A. Quintana, M. Sangesland, A. Castanza, L. Uhde, J. Hui, V. Z. Wall, A. Gagnidze, K. Oh, B. M. Wasko, F. J. Ramos, R. D. Palmiter, P. S. Rabinovitch, P. G. Morgan, M. M. Sedensky and M. Kaeberlein (2013). "mTOR inhibition alleviates mitochondrial disease in a mouse model of Leigh syndrome." Science **342**(6165): 1524-1528.

Kanamori, K. S., G. C. de Oliveira, M. Auxiliadora-Martins, R. A. Schoon, J. M. Reid and E. N. Chini (2018). "Two Different Methods of Quantification of Oxidized Nicotinamide Adenine Dinucleotide (NAD(+)) and Reduced Nicotinamide Adenine Dinucleotide (NADH) Intracellular Levels: Enzymatic Coupled Cycling Assay and Ultra-performance Liquid Chromatography (UPLC)-Mass Spectrometry." Bio Protoc **8**(14).

Kataura, T., L. Sedlackova, E. G. Otten, R. Kumari, D. Shapira, F. Scialo, R. Stefanatos, K. I. Ishikawa, G. Kelly, E. Seranova, C. Sun, D. Maetzel, N. Kenneth, S. Trushin, T. Zhang, E. Trushina, C. C. Bascom, R. Tasseff, R. J. Isfort, J. E. Oblong, S. Miwa, M. Lazarou, R. Jaenisch, M. Imoto, S. Saiki, M. Papamichos-Chronakis, R. Manjithaya, O. D. K. Maddocks, A. Sanz, S. Sarkar and V. I. Korolchuk (2022). "Autophagy promotes cell survival by maintaining NAD levels." Dev Cell **57**(22): 2584-2598 e2511.

Kemppainen, E., J. George, G. Garipler, T. Tuomela, E. Kiviranta, T. Soga, C. D. Dunn and H. T. Jacobs (2016). "Mitochondrial Dysfunction Plus High-Sugar Diet Provokes a Metabolic Crisis That Inhibits Growth." PLoS One **11**(1): e0145836.

Kemppainen, K. K., J. Rinne, A. Sriram, M. Lakanmaa, A. Zeb, T. Tuomela, A. Popplestone, S. Singh, A. Sanz, P. Rustin and H. T. Jacobs (2014). "Expression of alternative oxidase in Drosophila ameliorates diverse phenotypes due to cytochrome oxidase deficiency." Hum Mol Genet **23**(8): 2078-2093.

Leader, D. P., S. A. Krause, A. Pandit, S. A. Davies and J. A. T. Dow (2018). "FlyAtlas 2: a new version of the Drosophila melanogaster expression atlas with RNA-Seq, miRNA-Seq and sex-specific data." Nucleic Acids Res **46**(D1): D809-D815.

Lesner, N. P., X. Wang, Z. Chen, A. Frank, C. J. Menezes, S. House, S. D. Shelton, A. Lemoff, D. G. McFadden, J. Wansapura, R. J. DeBerardinis and P. Mishra (2022). "Differential requirements for mitochondrial electron transport chain components in the adult murine liver." Elife **11**.

Lopez-Otin, C., M. A. Blasco, L. Partridge, M. Serrano and G. Kroemer (2023). "Hallmarks of aging: An expanding universe." Cell **186**(2): 243-278.

O'Hanlon, M. E., C. Tweedy, F. Scialo, R. Bass, A. Sanz and T. K. Smulders-Srinivasan (2022). "Mitochondrial electron transport chain defects modify Parkinson's disease phenotypes in a Drosophila model." Neurobiol Dis **171**: 105803.

Obata, F., C. O. Fons and A. P. Gould (2018). "Early-life exposure to low-dose oxidants can increase longevity via microbiome remodelling in Drosophila." Nat Commun **9**(1): 975.

Owusu-Ansah, E., W. Song and N. Perrimon (2013). "Muscle mitohormesis promotes longevity via systemic repression of insulin signaling." Cell **155**(3): 699-712.

Pirinen, E., M. Auranen, N. A. Khan, V. Brilhante, N. Urho, A. Pessia, A. Hakkarainen, J. K. Ulla Heinonen, M. S. Schmidt, K. Haimilahti, P. Piirila, N. Lundbom, M. R. Taskinen, C. Brenner, V. Velagapudi, K. H. Pietilainen and A. Suomalainen (2020). "Niacin Cures Systemic NAD(+) Deficiency and Improves Muscle Performance in Adult-Onset Mitochondrial Myopathy." Cell Metab **32**(1): 144.

Rimal, S., I. Tantray, Y. Li, T. Pal Khaket, Y. Li, S. Bhurtel, W. Li, C. Zeng and B. Lu (2023). "Reverse electron transfer is activated during aging and contributes to aging and age-related disease." EMBO Rep: e55548.

Scialo, F., A. Sriram, D. Fernandez-Ayala, N. Gubina, M. Lohmus, G. Nelson, A. Logan, H. M. Cooper, P. Navas, J. A. Enriquez, M. P. Murphy and A. Sanz (2016). "Mitochondrial ROS Produced via Reverse Electron Transport Extend Animal Lifespan." Cell Metab **23**(4): 725-734.
Stefanatos, R., F. Robertson, A. H. Uribe, Y. Yu, K. Myers, B. Castejon-Vega, T. Kataura, L. M. Martins, V. I. Korolchuk, O. D. K. Maddocks and A. Sanz (2023). "Developmental mitochondrial Complex I activity determines lifespan." bioRxiv: 2023.2006.2021.545894.
Wallace, D. C. (2005). "A mitochondrial paradigm of metabolic and degenerative diseases, aging, and cancer: a dawn for evolutionary medicine." Annu Rev Genet **39**: 359-407.
Wang, A., J. Mouser, J. Pitt, D. Promislow and M. Kaeberlein (2016). "Rapamycin enhances survival in a Drosophila model of mitochondrial disease." Oncotarget **7**(49): 80131-80139.

Figure Legends

Figure 1. Developmental Depletion of Respiratory Complex IV Profoundly Reduces Adult Lifespan. (A) Diagrammatic representation of the experimental interventions employed to deplete CIV either during developmental stages or encompassing both developmental and adult stages. (B) Lifespan analysis, illustrated through survival curves, of specified genotypes. (D-G) qPCR assessment of mRNA expression levels for selected genes, with specified genotypes and life stages. Data is presented as mean ± SEM. (H-I) Violin plots demonstrating mitochondrial oxygen consumption rates across indicated phenotypes. * $p < 0.05$.

Figure S1. Supplementary to Figure 1. (A) Lifespan examination, depicted through survival curves, for COX4 flies subjected to varying concentrations of RU-486 during development. (B-C) Mortality rates explored through Gompertz analysis for the indicated genotypes. Regression lines fitting to the mortality data provide a visual representation of the probability of death over time as predicted by the Gompertz model. (D) Lifespan investigation, illustrated via survival curves, for specified genotypes. (E-F) qPCR evaluation of mRNA levels of chosen genes, with identified genotypes and life stages.

Figure 2. Developmental depletion of CIV triggers transcriptomic reconfiguration, dysregulating fatty acid metabolism in adults. (A) Diagrammatic representation of the transcriptomic analysis conducted. (B) PCA plot illustrating the variance and clustering of the short- and long-lived groups, with genotypes as indicated within the figure. (C) Volcano plot visualising DEGs when contrasting short-lived and long-lived COX5 flies. (D) Dot plot illustrating the three most significantly impacted pathways within each specified category, as identified through GO and KEGG analysis. (E) Volcano plots illustrating the most significantly enriched genes in each indicated fly tissue, according to

FlyAtlas data. (F) Venn diagrams illustrating the unique and shared upregulated (upper diagram) and downregulated (lower diagram) genes in short-lived flies with depletion of either CI or CIV.

Figure S2. Supplementary to Figure 2. (A) Volcano plot portraying DEGs in a comparison between short-lived and long-lived control flies. (B) A series of volcano plots showcasing the most significantly enriched genes in each specified fly tissue, as per FlyAtlas data. C-D) Gene Set Enrichment Analysis (GSEA) plots revealing significant gene expression patterns corresponding with the specific biological terms.

Figure 3. Developmental depletion of CIV disrupts fat storing and interrupts TOR signalling in adults. (A) Representative confocal microscopy images of the fat body in specified groups: I = Long-lived control; II = Short-lived control; III = Long-lived COX5B; IV = Short-lived COX5B. (B) Box and whisker plots indicating TAG levels across specified genotypes, displaying median, minimum, and maximum values. (C) Survival curve illustrating the lifespan of flies under starvation conditions for indicated phenotypes. (D) Representative Western blot analysis for indicated protein in specified genotypes. (E) Quantification corresponding to panel D. (F) Representative Western blot analysis for indicated protein in specified genotypes. (G) Quantitative analysis corresponding to panel F. E and G show mean ± SEM (H) Violin plots showing assessment of NAD+ and NADH levels across specified genotypes. * $p<0.05$, *** $p<0.001$

Figure S3. Supplementary to Figure 3. (A) Box and whisker plot indicating TAG levels across specified genotypes, displaying median, minimum, and maximum values. (B) Survival curve illustrating the lifespan of flies under starvation conditions for indicated phenotypes. (C-D) Survival curve illustrating the lifespan of flies fed with H_2O_2 for indicated phenotypes. (E-F) Survival curve illustrating the lifespan of flies under thermal

stress conditions for indicated phenotypes. (G) Violin plots showing assessment of NAD+ and NADH levels across specified phenotypes.

Figure 4. Targeted rescue of mitochondrial function during development improves energetic balance in adults. (A) Diagrammatic representation of how AOX reinstates electron flow upon CIV depletion. (B) PCA plot illustrating the variance and clustering of the short- and long-lived groups, with genotypes as indicated within the figure. (C) Dot plot illustrating the three most significantly impacted pathways within each specified category, as identified through GO analysis. (D-E) Volcano plots depicting DEGs when comparing short-lived COX5 flies with long-lived COX5B (D) and AOX active (E). Genes displayed in the plot correspond to those with fat-body larval stage-limited expression. (F) Survival curve illustrating the lifespan of flies under starvation conditions for indicated phenotypes.

Figure S4. Supplementary to Figure 4. (A) Heatmap depicting genes with restored expression due to developmental AOX activity. (B-D) Survival curve illustrating the lifespan of flies under starvation conditions for indicated genotypes. (E) Representative confocal microscopy images of the fat body in specified groups: I = Long-lived COX5B; II = AOX inactive; III = Short-lived COX5B; IV = AOX active. (F) Box and whisker plot indicating TAG levels across specified genotypes, displaying median, minimum, and maximum values. Significance values are provided in the figure.

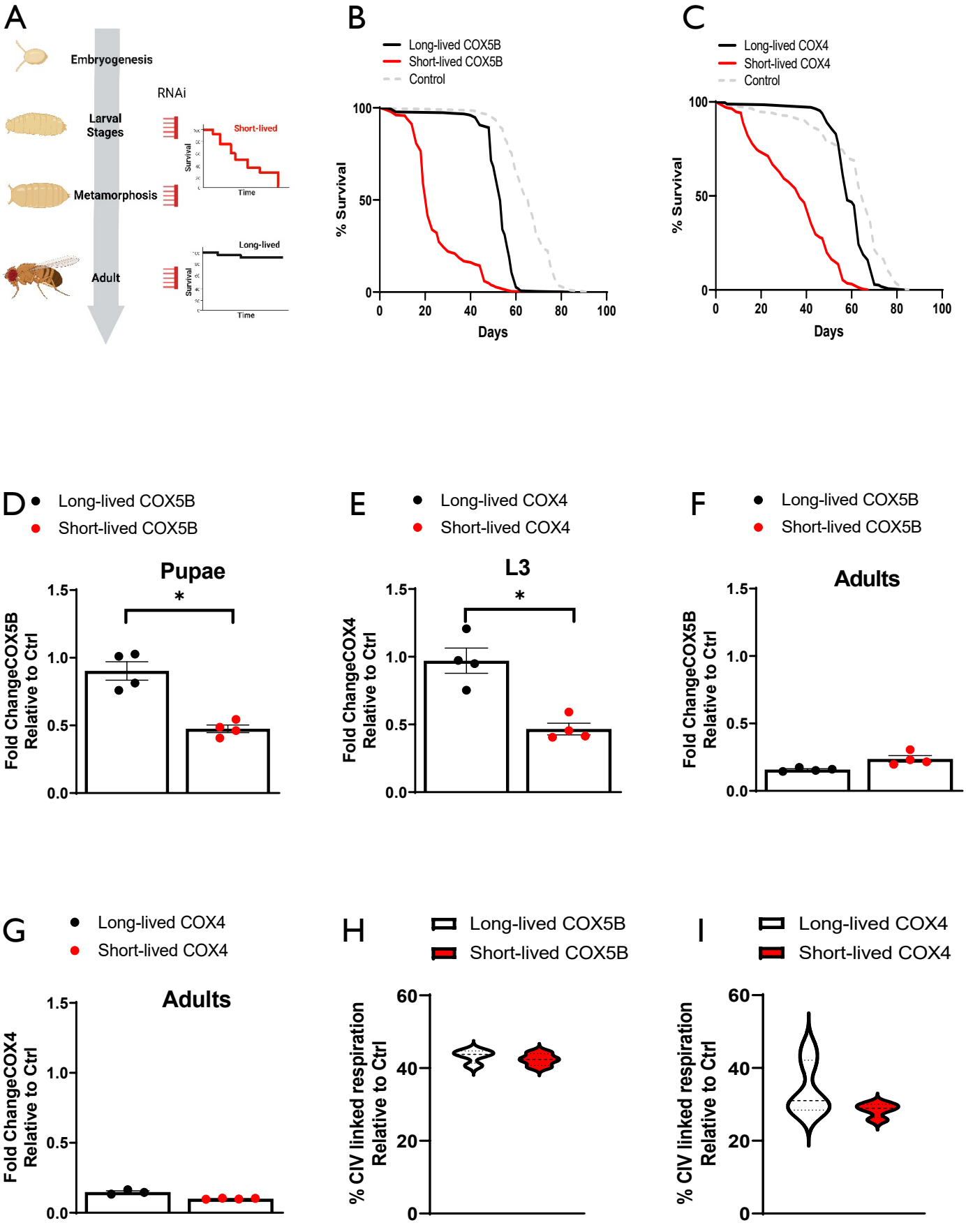
A
Embryogenesis
Larval Stages
Metamorphosis
Adult
RNAi
Short-lived
Long-lived
Survival
Time
B
Long-lived COX5B
Short-lived COX5B
Control
% Survival
Days
C
Long-lived COX4
Short-lived COX4
Control
% Survival
Days
D
Long-lived COX5B
Short-lived COX5B
Pupae
Fold ChangeCOX5B Relative to Ctrl
E
Long-lived COX4
Short-lived COX4
L3
Fold ChangeCOX4 Relative to Ctrl
F
Long-lived COX5B
Short-lived COX5B
Adults
Fold ChangeCOX5B Relative to Ctrl
G
Long-lived COX4
Short-lived COX4
Adults
Fold ChangeCOX4 Relative to Ctrl
H
Long-lived COX5B
Short-lived COX5B
% CIV linked respiration Relative to Ctrl
I
Long-lived COX4
Short-lived COX4
% CIV linked respiration Relative to Ctrl

Figure 1

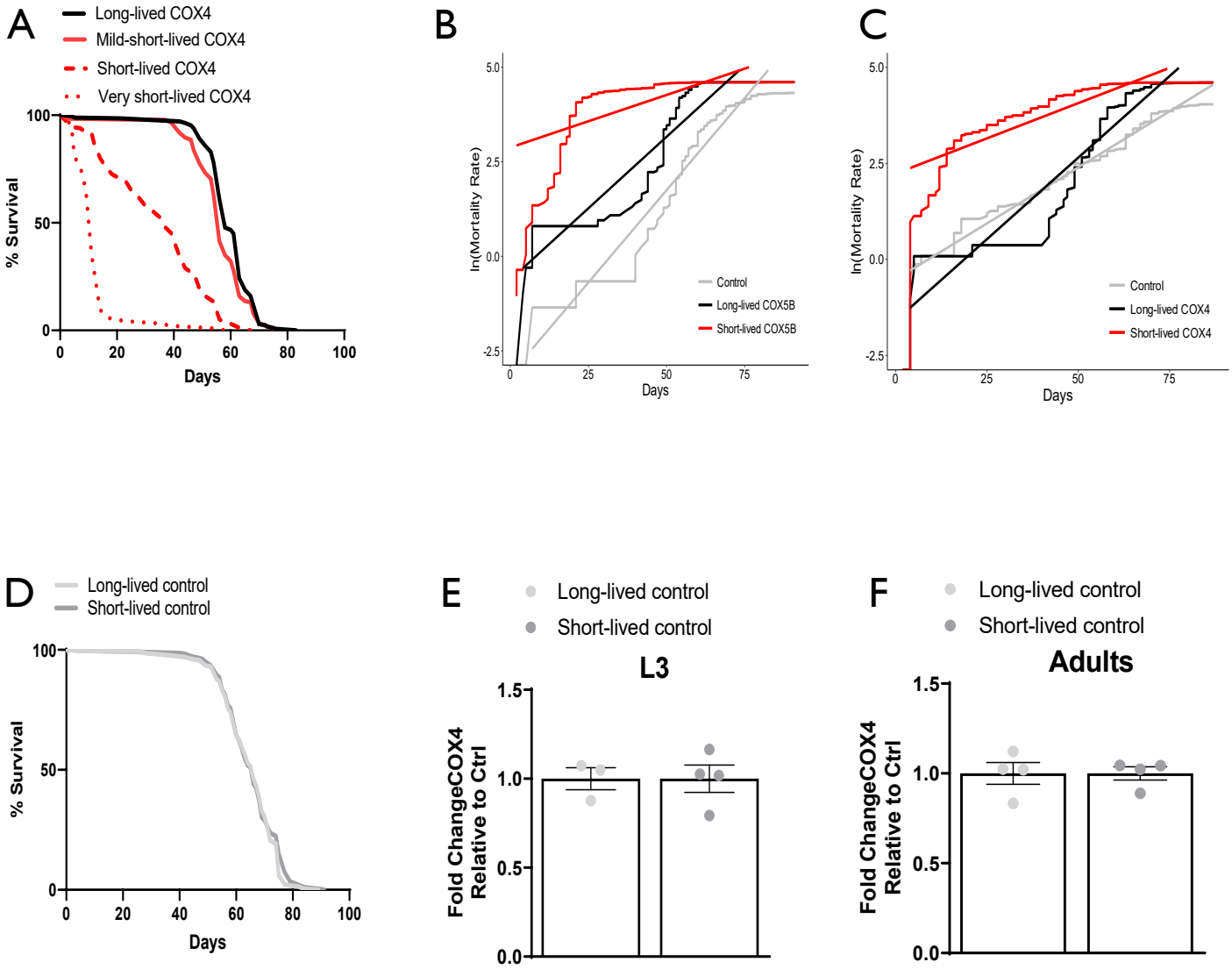
A
Long-lived COX4
Mild-short-lived COX4
Short-lived COX4
Very short-lived COX4
% Survival
Days
B
ln(Mortality Rate)
Control
Long-lived COX5B
Short-lived COX5B
Days
C
ln(Mortality Rate)
Control
Long-lived COX4
Short-lived COX4
Days
D
Long-lived control
Short-lived control
% Survival
Days
E
Long-lived control
Short-lived control
L3
Fold ChangeCOX4 Relative to Ctrl
F
Long-lived control
Short-lived control
Adults
Fold ChangeCOX4 Relative to Ctrl

Figure S1

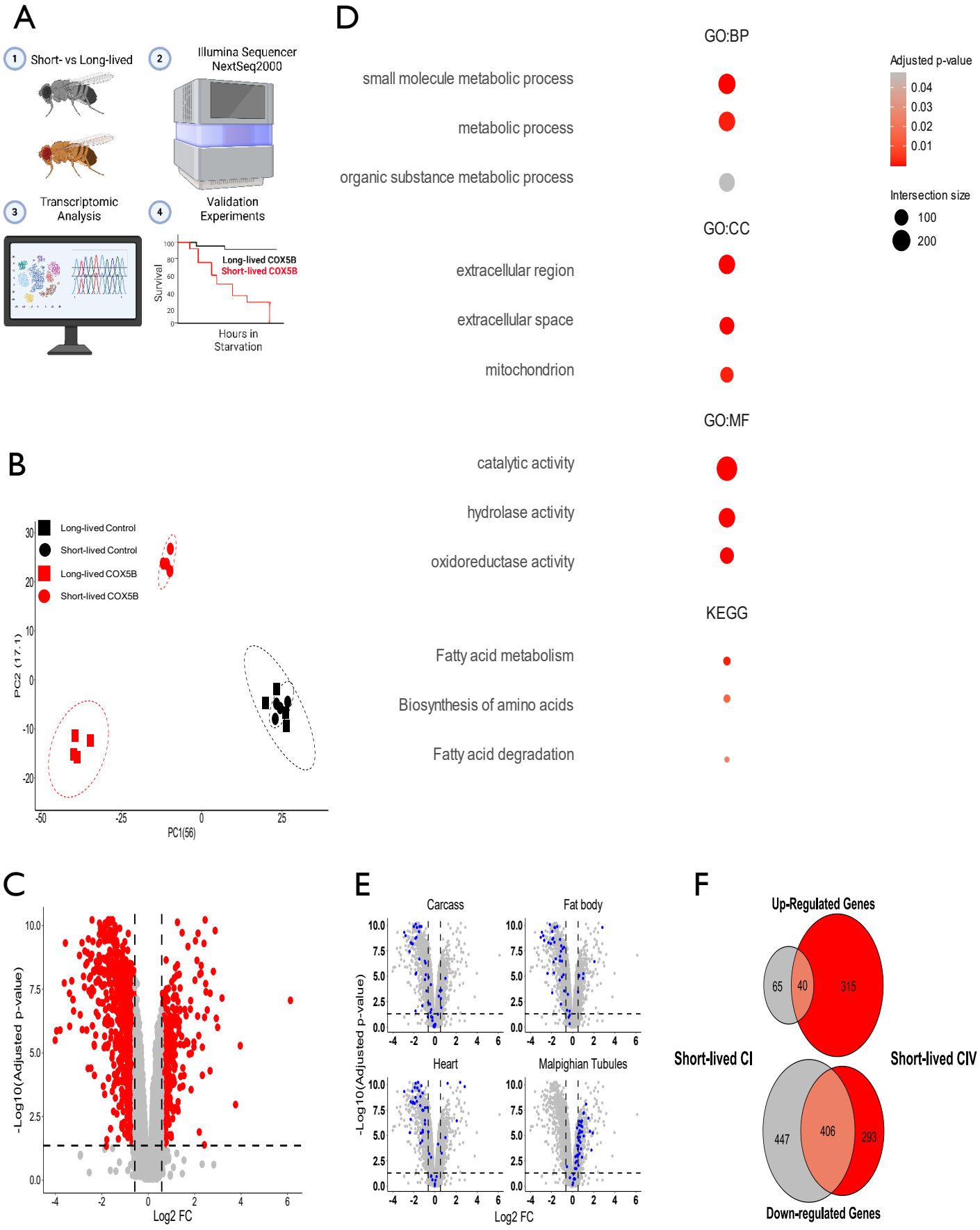
A
1 Short- vs Long-lived
2 Illumina Sequencer NextSeq2000
3 Transcriptomic Analysis
4 Validation Experiments
Long-lived COX5B
Short-lived COX5B
Survival
Hours in Starvation
B
Long-lived Control
Short-lived Control
Long-lived COX5B
Short-lived COX5B
PC2 (17.1)
PC1(56)
C
-Log10(Adjusted p-value)
Log2 FC
D
GO:BP
small molecule metabolic process
metabolic process
organic substance metabolic process
GO:CC
extracellular region
extracellular space
mitochondrion
GO:MF
catalytic activity
hydrolase activity
oxidoreductase activity
KEGG
Fatty acid metabolism
Biosynthesis of amino acids
Fatty acid degradation
Adjusted p-value
0.04
0.03
0.02
0.01
Intersection size
100
200
E
Carcass
Fat body
Heart
Malpighian Tubules
-Log10(Adjusted p-value)
Log2 FC
F
Up-Regulated Genes
65
40
315
Short-lived CI
Short-lived CIV
447
406
293
Down-regulated Genes

Figure 2

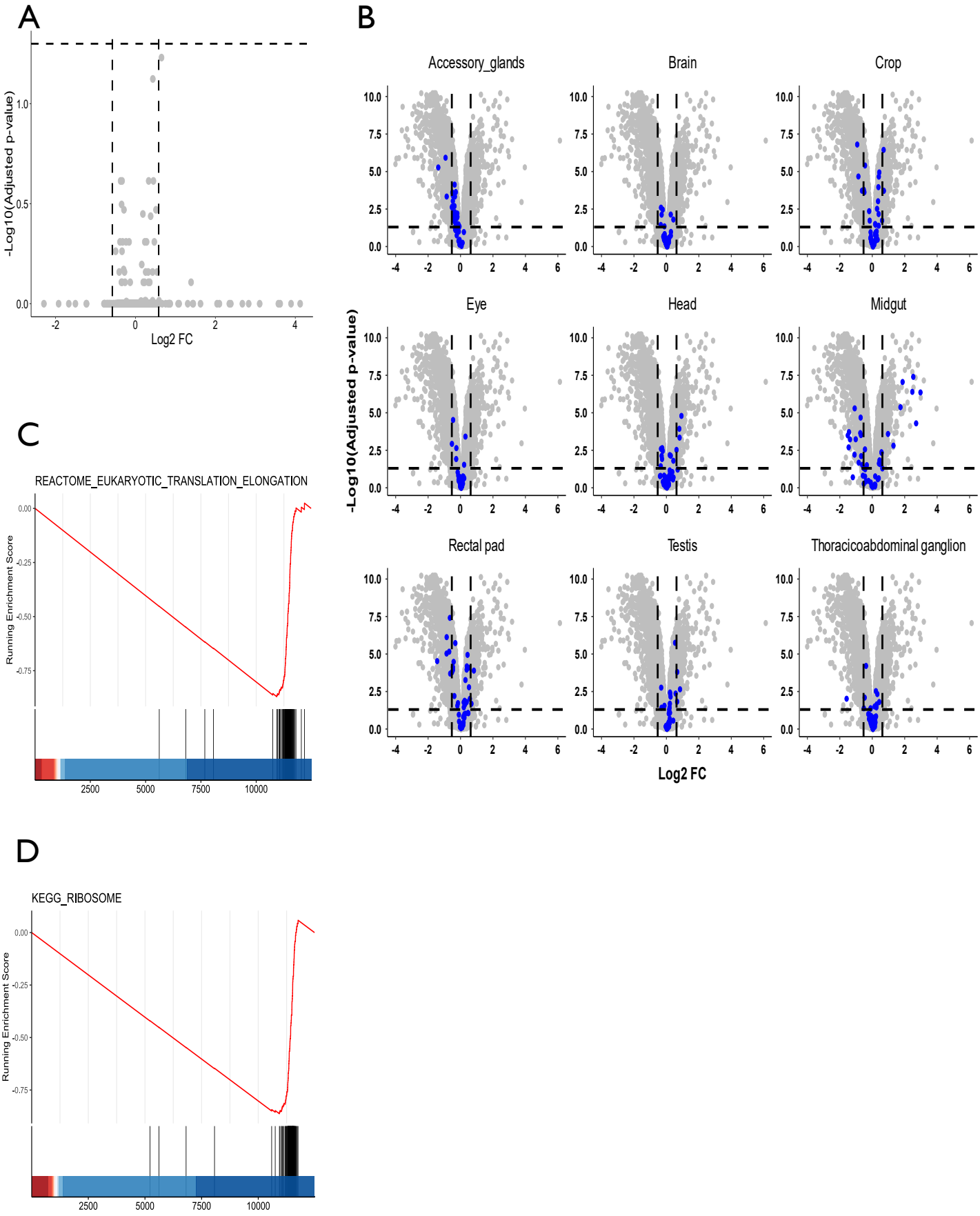
A
-Log10(Adjusted p-value)
Log2 FC
B
Accessory_glands
Brain
Crop
Eye
Head
Midgut
Rectal pad
Testis
Thoracicoabdominal ganglion
-Log10(Adjusted p-value)
Log2 FC
C
REACTOME_EUKARYOTIC_TRANSLATION_ELONGATION
Running Enrichment Score
D
KEGG_RIBOSOME
Running Enrichment Score

Figure S2

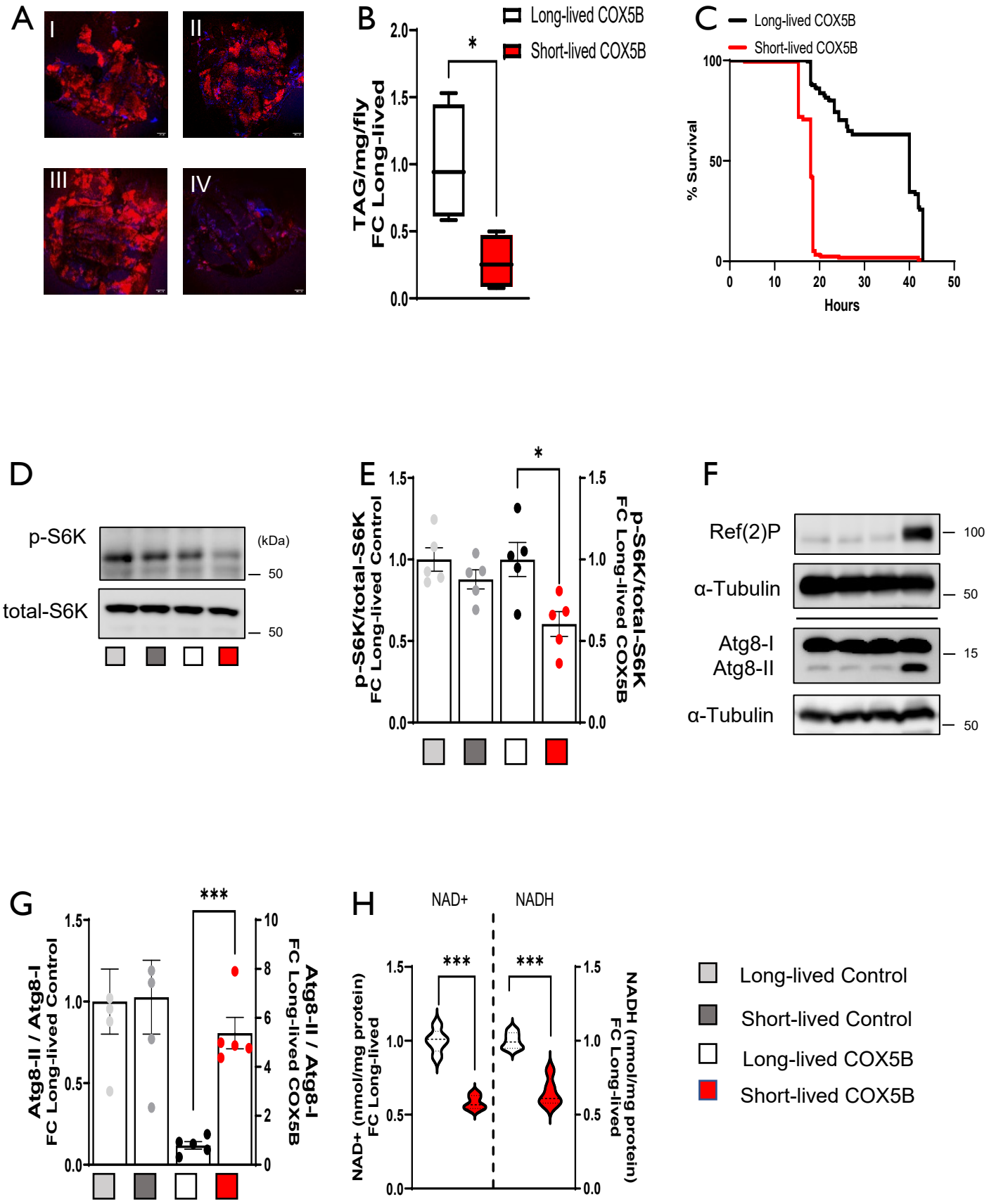
A
I
II
III
IV
B
Long-lived COX5B
Short-lived COX5B
TAG/mg/fly
FC Long-lived
2.0
1.5
1.0
0.5
0.0
*
C
Long-lived COX5B
Short-lived COX5B
% Survival
100
50
0
0
10
20
30
40
50
Hours
D
p-S6K
total-S6K
(kDa)
50
50
E
p-S6K/total-S6K
FC Long-lived Control
p-S6K/total-S6K
FC Long-lived COX5B
1.5
1.0
0.5
0.0
*
F
Ref(2)P
α-Tubulin
Atg8-I
Atg8-II
α-Tubulin
100
50
15
50
G
Atg8-II / Atg8-I
FC Long-lived Control
Atg8-II / Atg8-I
FC Long-lived COX5B
1.5
1.0
0.5
0.0
10
8
6
4
2
0
***
H
NAD+
NADH
NAD+ (nmol/mg protein)
FC Long-lived
NADH (nmol/mg protein)
FC Long-lived
1.5
1.0
0.5
0.0
***
***
Long-lived Control
Short-lived Control
Long-lived COX5B
Short-lived COX5B

Figure 3

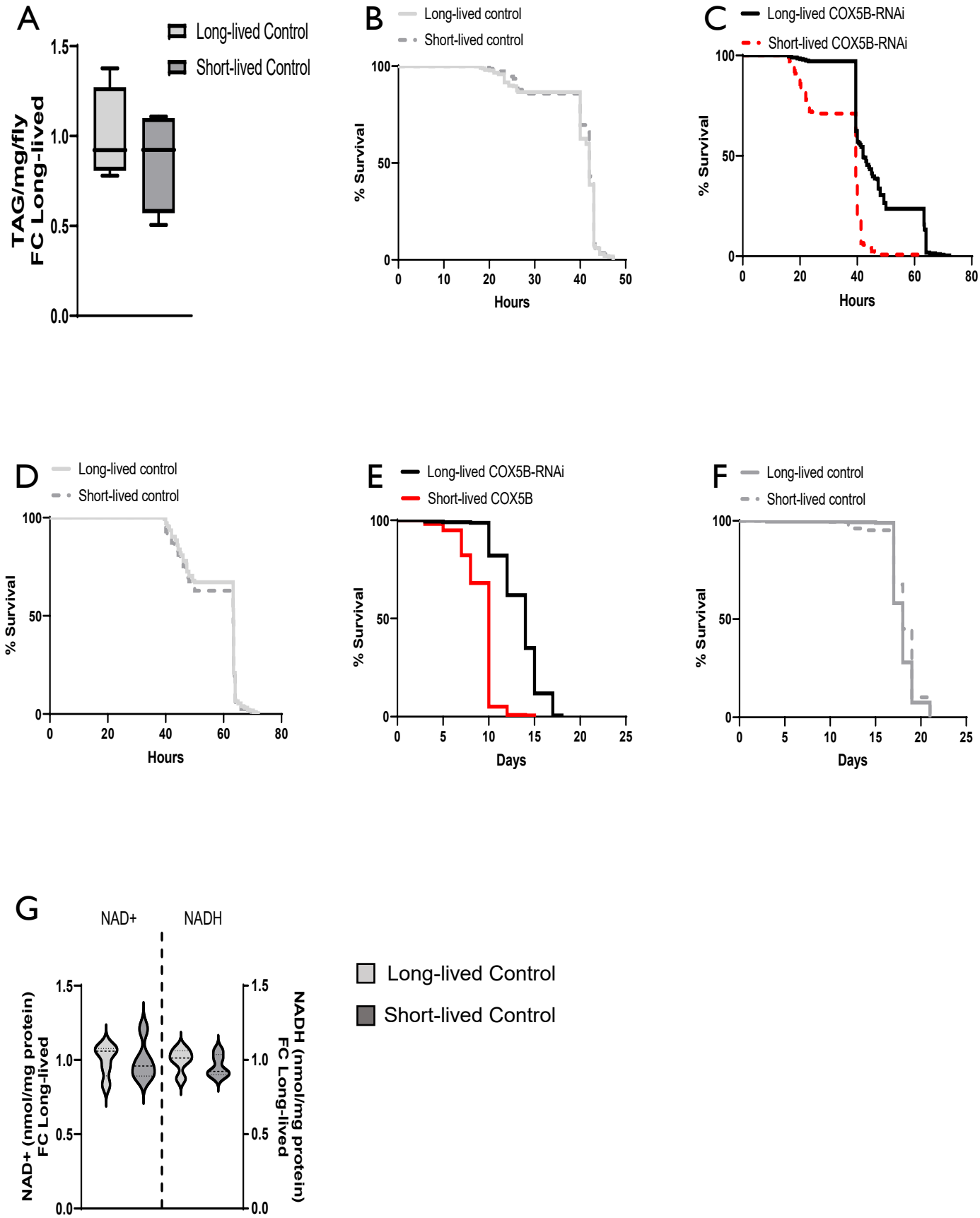
A
Long-lived Control
Short-lived Control
TAG/mg/fly
FC Long-lived
1.5
1.0
0.5
0.0
B
Long-lived control
Short-lived control
% Survival
100
50
0
0
10
20
30
40
50
Hours
C
Long-lived COX5B-RNAi
Short-lived COX5B-RNAi
% Survival
100
50
0
0
20
40
60
80
Hours
D
Long-lived control
Short-lived control
% Survival
100
50
0
0
20
40
60
80
Hours
E
Long-lived COX5B-RNAi
Short-lived COX5B
% Survival
100
50
0
0
5
10
15
20
25
Days
F
Long-lived control
Short-lived control
% Survival
100
50
0
0
5
10
15
20
25
Days
G
NAD+
NADH
NAD+ (nmol/mg protein)
FC Long-lived
NADH (nmol/mg protein)
FC Long-lived
1.5
1.0
0.5
0.0
Long-lived Control
Short-lived Control

Figure S3

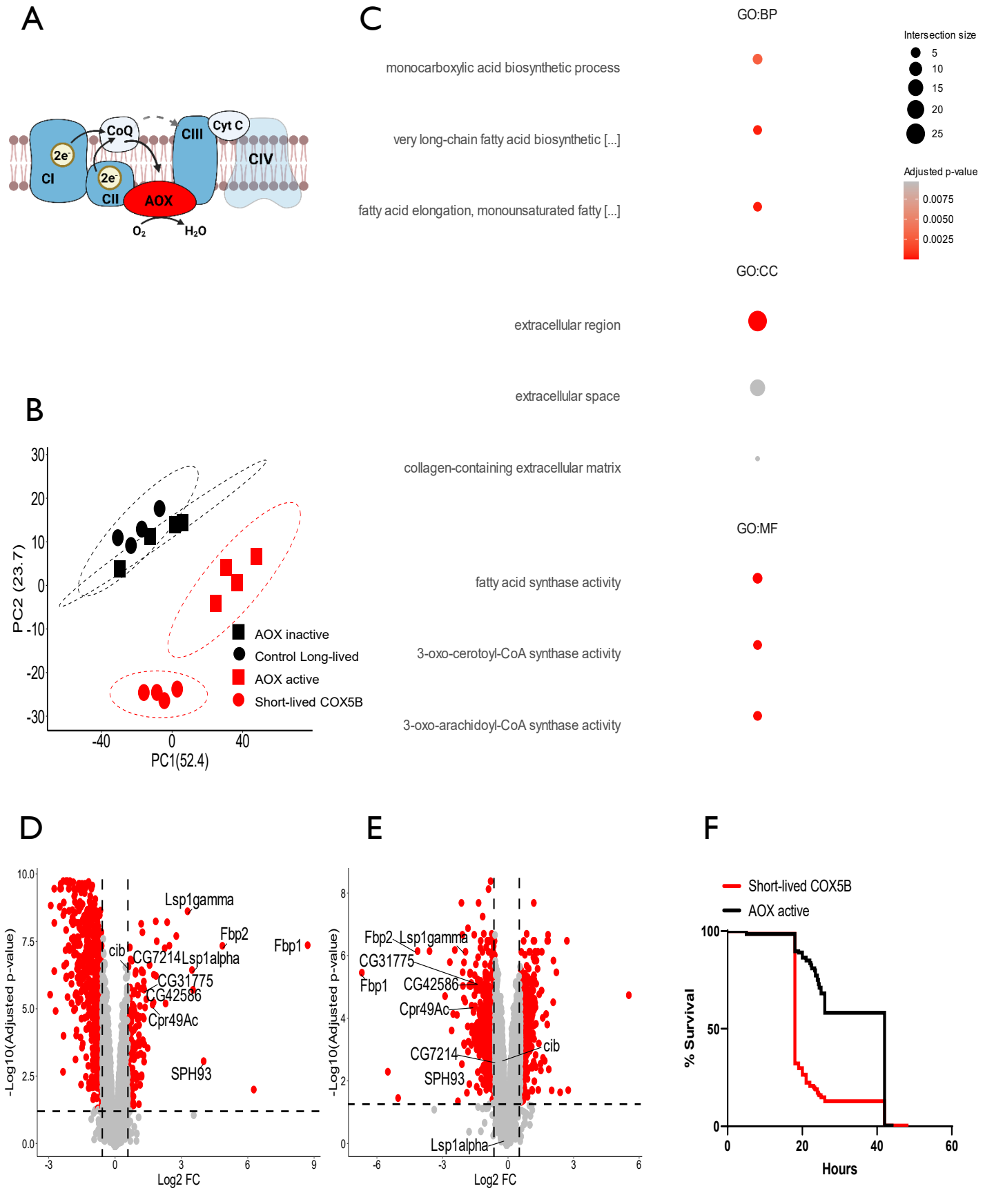
A
CoQ
CIII
Cyt C
CIV
CI
CII
AOX
2e⁻
2e⁻
O2
H2O
B
PC2 (23.7)
PC1(52.4)
AOX inactive
Control Long-lived
AOX active
Short-lived COX5B
C
GO:BP
monocarboxylic acid biosynthetic process
very long-chain fatty acid biosynthetic [...]
fatty acid elongation, monounsaturated fatty [...]
GO:CC
extracellular region
extracellular space
collagen-containing extracellular matrix
GO:MF
fatty acid synthase activity
3-oxo-cerotoyl-CoA synthase activity
3-oxo-arachidoyl-CoA synthase activity
Intersection size
5
10
15
20
25
Adjusted p-value
0.0075
0.0050
0.0025
D
-Log10(Adjusted p-value)
Log2 FC
Lsp1gamma
Fbp2
Fbp1
cib
CG7214
Lsp1alpha
CG31775
CG42586
Cpr49Ac
SPH93
E
-Log10(Adjusted p-value)
Log2 FC
Fbp2
Lsp1gamma
CG31775
Fbp1
CG42586
Cpr49Ac
CG7214
cib
SPH93
Lsp1alpha
F
Short-lived COX5B
AOX active
% Survival
Hours

Figure 4

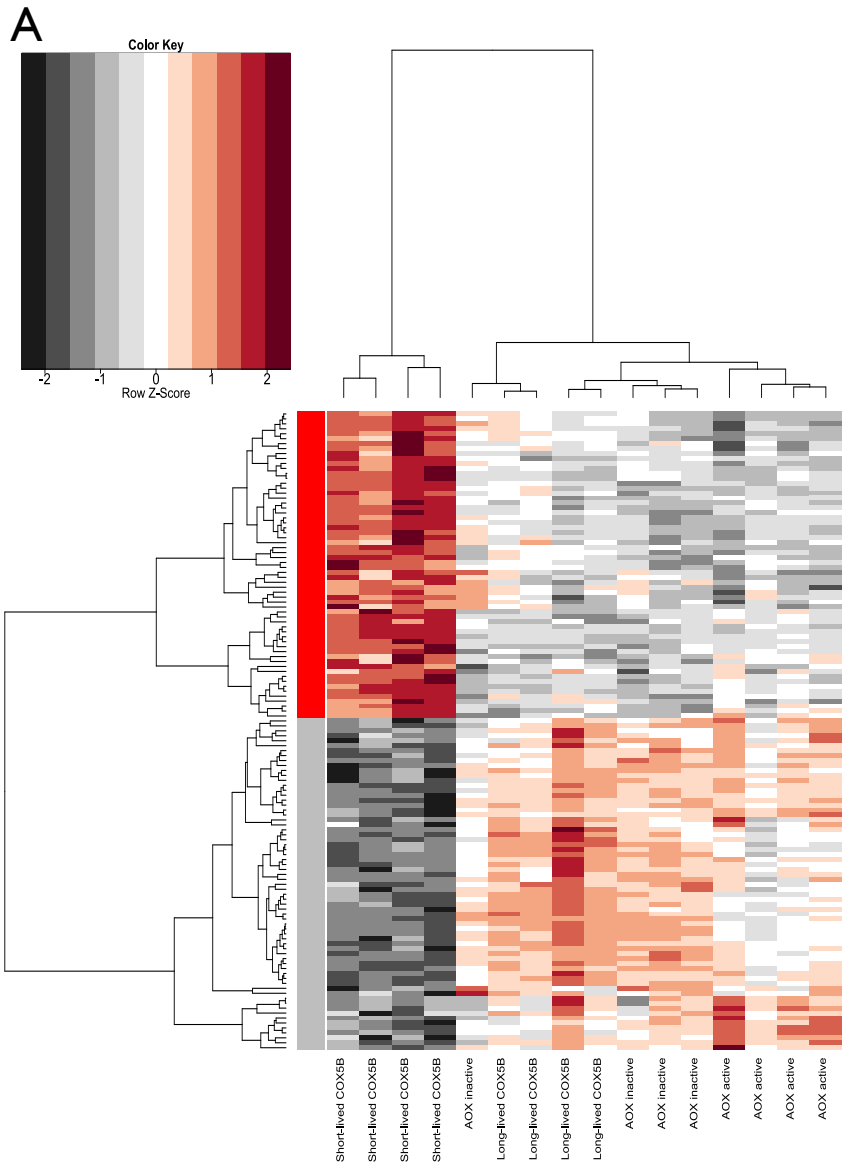
A
Color Key
-2
-1
0
1
2
Row Z-Score
Short-lived COX5B
Short-lived COX5B
Short-lived COX5B
Short-lived COX5B
AOX inactive
Long-lived COX5B
Long-lived COX5B
Long-lived COX5B
Long-lived COX5B
AOX inactive
AOX inactive
AOX inactive
AOX active
AOX active
AOX active
AOX active

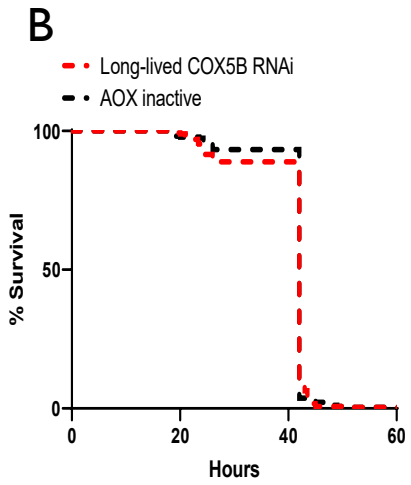
B
Long-lived COX5B RNAi
AOX inactive
% Survival
100
50
0
0
20
40
60
Hours

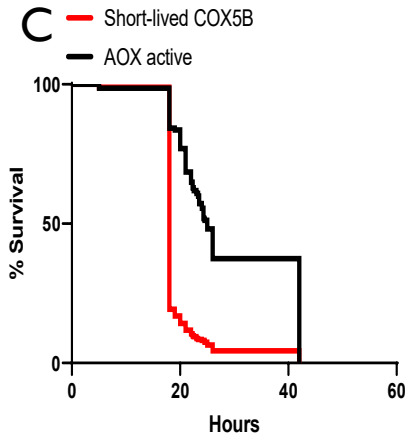
C
Short-lived COX5B
AOX active
% Survival
100
50
0
0
20
40
60
Hours

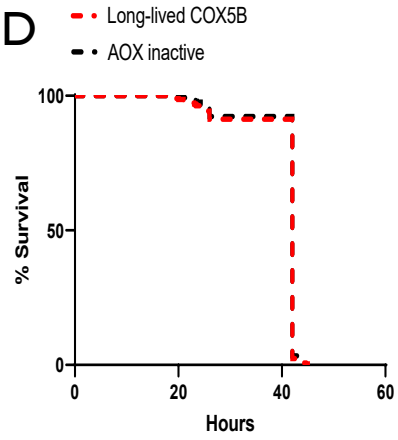
D
Long-lived COX5B
AOX inactive
% Survival
100
50
0
0
20
40
60
Hours

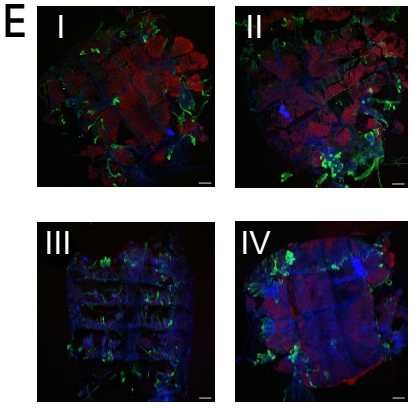
E
I
II
III
IV

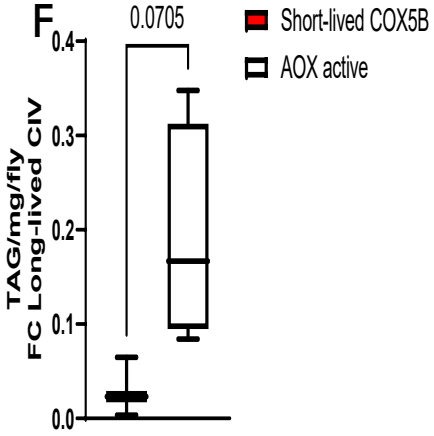
F
0.0705
Short-lived COX5B
AOX active
TAG/mg/fly
FC Long-lived CIV
0.4
0.3
0.2
0.1
0.0

Figure S4